Influence of the layer parameters on the performance of the CdTe solar cells

Assiya Haddout*, Abderrahim Raidou, and Mounir Fahoume

Laboratory of Condensed Matter Physics, Department of Physics, Faculty of Science, Ibn Tofail University, Kenitra BP 133-14000, Morocco

(Received 23 October 2017; Revised 25 November 2017)

Influence of the layer parameters on the performances of the CdTe solar cells is analyzed by SCAPS-1D. The ZnO: Al film shows a high efficiency than SnO_2:F. Moreover, the thinner window layer and lower defect density of CdS films are the factor in the enhancement of the short-circuit current density. As well, to increase the open-circuit voltage, the responsible factors are low defect density of the absorbing layer CdTe and high metal work function. For the low cost of cell production, ultrathin film CdTe cells are used with a back surface field (BSF) between CdTe and back contact, such as PbTe. Further, the simulation results show that the conversion efficiency of 19.28% can be obtained for the cell with 1-μm-thick CdTe, 0.1-μm-thick PbTe and 30-nm-thick CdS.

Document code: A **Article ID:** 1673-1905(2018)02-0098-6

DOI https://doi.org/10.1007/s11801-018-7229-4

After several years of research and development, thin-film solar cells are attracting increasing interest. The polycrystalline thin film CdTe/CdS heterojunction has drawn significant attention to achieve better efficiency and cost ratio because of its facile adaptability to large-scale manufacturing processes, and it is an alternative to the silicon solar cell. CdTe is an absorbing semiconductor for the solar cell with excellent electronic property, high optical absorption coefficient of the order of 10^5 cm^{-1}, direct bandgap energy of 1.45 eV which is very close to the optimum bandgap for solar cells, and the theoretical efficiency reaching around 29%[1]. National Renewable Energy Laboratory reported a conversion efficiency η of 16.7% with open-circuit voltage V_{OC} of 0.84 V, short-circuit density J_{SC} of 26.1 mA/cm^2, fill factor (FF) of 75.5% for area of 1.032 cm^2 in 2010[2], and then reported a conversion efficiency η of 21.0% with V_{OC}=0.87 V, J_{SC}=30.25 mA/cm^2 and FF=79.4% for area of 1.062 3 cm^2 in 2016[3].

The simulation software of Solar Cell Capacitance Simulator-1 Dimension (SCAPS-1D) is able to solve the basic semiconductor equations which are the Poisson equation and the continuity equations for electrons and holes[4]. Several researchers have used the simulation software to improve the conversion efficiency of the CdS/CdTe solar cells. The researches about the impacts of the carrier lifetimes, carrier densities, back contact barriers, CdS film thickness, doping concentration, CdTe film thickness, back surface recombination velocity and electron reflector on the characteristics of CdTe solar cells were reported[5,6] .

In this paper, we simulate CdTe solar cells by using SCAPS-1D software. We study the influence of CdS films thickness, the defect density and back metal work function on performance of CdTe solar cells with ZnO:Al as front contact. Moreover, we study the current density-voltage curves of ultrathin film CdTe solar cell with 1 μm CdTe and 100 nm PbTe acting as back surface field (BSF).

The conventional structure SnO_2/CdS/CdTe has been used for more than 30 years. CdTe solar cells generally require a transparent front contact layer with high conductivity to facilitate current collection. Fluorine-doped tin oxide (SnO_2:F) is one of the few materials, which is robust enough for these devices. Britt and Ferekides[7] have used SnO_2:F to produce CdTe cells with 15.8% efficiency. The conventional SnO_2 has been replaced by cadmium stannate (Cd_2SnO_4 or CTO)[8] and Al-doped ZnO (ZnO:Al or AZO)[9]. However, CTO and AZO show excellent transparency over the entire visible spectrum than SnO_2:F. The CdTe solar cells produces with these different transparent conductive oxides (TCOs), and the results show that the highest efficiency of 16.5% can be achieved using CTO[8], and 14% can be achieved using AZO[9].

The conventional solar cells were modeled by Khosroabadi and Keshmiri[10], under AM 1.5G conditions, and this cell has the conversion efficiency of 15.11% with V_{OC}=0.88 V, J_{SC}=24.2 mA/cm^2 and FF=71.1%. In this paper, the conventional structure is the starting point for these investigations. Fig.1(a) shows the schematic structure of this cell, which is composed of 500-nm-thick SnO_2:F, 100-nm-thick CdS, 4-nm-thick CdTe and back contact. The computer simulation tool of SCAPS-1D was

* E-mail: assiyahd@gmail.com

employed for the simulation[11].

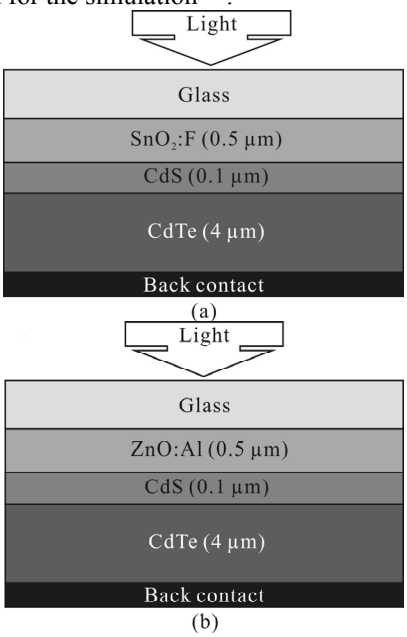

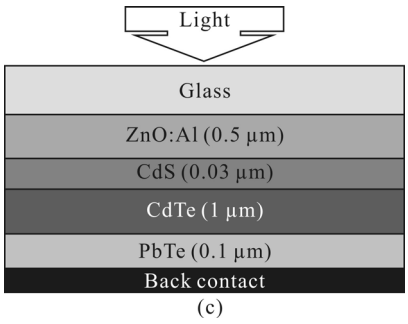

Fig.1 Structure of the CdTe solar cells: (a) Conventional baseline case structure; (b) Modified structure for higher conversion efficiency by ZnO:Al TCO layer; (c) Ultrathin cell with PbTe BSF layer

The baseline structure shown in Fig.1(a) is modified by using ZnO:Al (AZO) as a TCO front contact, and the properties of the other layers (CdS and CdTe) are fixed, as shown in Fig.1(b). The input parameters for the simulation are given in Tab.1.

Tab.1 The layer parameters used in CdTe solar cells, simulated by SCAPS-1D model[10-14]

General device properties			Front	Back
Surface recombination velocity for electron S_e (cm/s)			10^7	10^7
Surface recombination velocity for hole S_h (cm/s)			10^7	10^7
Metal work function (eV)			4.1	4.92
Reflectivity R_f			0.1	0.8
Layer properties	SnO_2:F/ZnO:Al	CdS	CdTe	PbTe
Thickness (μm)	0.5	0.01—0.1	4	0.1
Dielectric constant $\varepsilon/\varepsilon_0$	9	10	9.4	40
Bandgap energy E_g (eV)	3.6/3.35	2.40	1.5	0.29
Electron affinity χ (eV)	4/4.3	4.0	3.9	4.6
Electron mobility μ_e (cm^2/Vs)	100	100	320	1600
Hole mobility μ_h (cm^2/Vs)	25	25	40	600
Electron/Hole density n, p (cm^{-3})	n:10^{20}/10^{21}	n:10^{17}	p:2×10^{14}	8×10^{19}
Conduction band effective density of states N_C (cm^{-3})	2.2×10^{18}	2.2×10^{18}	8×10^{17}	1×10^{16}
Valence band effective density of states N_V (cm^{-3})	1.8×10^{19}	1.8×10^{19}	1.8×10^{19}	2×10^{17}
Electron capture cross section σ_e (cm^2)	10^{-12}	10^{-17}	10^{-12}	10^{-11}
Hole capture cross section σ_h (cm^2)	10^{-15}	10^{-12}	10^{-15}	10^{-16}
Defect density N_{AG}, N_{DG} (cm^{-3})	N_{AG}:10^{15}	N_{AG}:10^{15}	N_{DG}:2×10^{14}	N_{DG}:10^{16}

The typical current density-voltage characteristic curves for baseline structure with SnO_2:F and advanced structure with ZnO:Al of CdTe solar cell are shown in Fig.2(a). The comparison in Fig.2(a) shows that the major difference between these two types of cells is the higher current density achieved with the ZnO:Al (AZO). V_{OC} and FF are almost the same for these two devices. The efficiency of the device is increased from 15.14% to 16.36% entirely due to the increased J_{SC} from 24.62 mA to 26.55 mA because of higher transmission of AZO in the visible region.

Fig.2(b) shows the band diagram of the advanced solar cell with ZnO:Al (TCO) front contact. The interface of the heterojunction n-CdS/p-CdTe shows a discontinuity of the conduction bands ΔE_C of 0.1 eV and the valence bands ΔE_V of 0.9 eV.

The CdTe/CdS solar cells have demonstrated the highest performance to date, the bandgap energy of CdS window layer is 2.42 eV, and 0.1-μm-thick CdS absorbs about 63% of the incident radiation with energy greater than the bandgap energy. Thus, the use of CdS films with small thicknesses is desirable in order to maximize the photocurrent from the absorber[15]. The improvement of short-circuit current density results from the improved proprieties of CdS film. The effect of CdS layer thickness changing from 10 nm to 100 nm on the cell output parameters is shown in the Fig.3. When reducing the thickness of CdS layer (<30 nm), the efficiency of the cell is increased due to the increase of short-circuit current density J_{SC}, without compromising FF and V_{OC}, as shown in Fig.3.

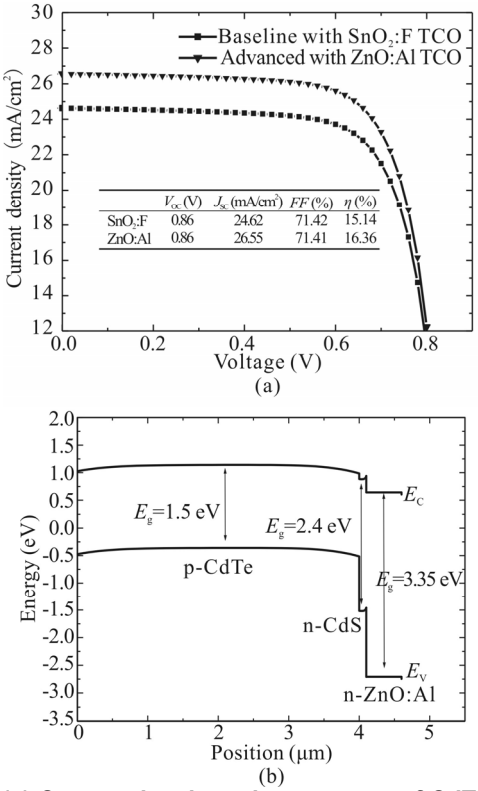

	V_{oc} (V)	J_{sc} (mA/cm^2)	FF (%)	η (%)
SnO_2:F	0.86	24.62	71.42	15.14
ZnO:Al	0.86	26.55	71.41	16.36

Fig.2 (a) Current density-voltage curves of CdTe solar cells on SnO_2:F and ZnO:Al; (b) Band diagram of CdTe solar cells on ZnO:Al

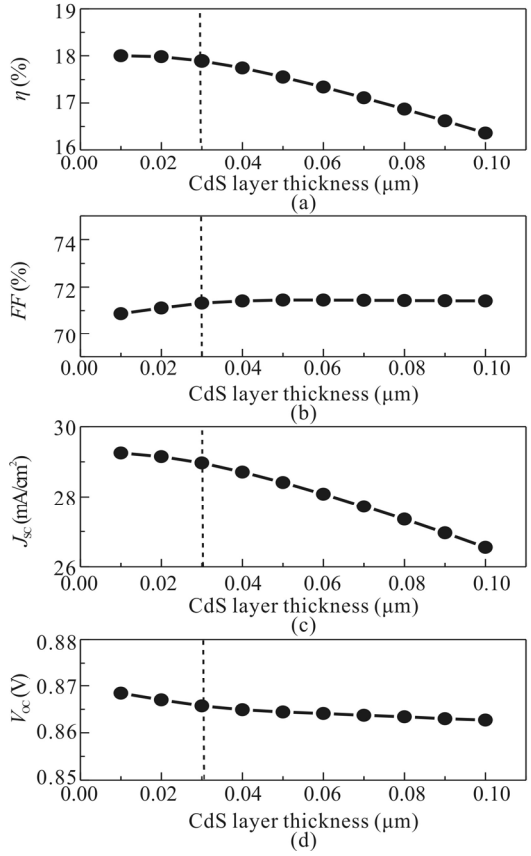

Fig.3 Thickness effect of CdS window layer on solar cell parameters

In addition, the performance for the defect density of CdS films varying from 10^{14} cm^{-3} to 10^{17} cm^{-3} is shown in Fig.4. When reducing the defect density of CdS layer from 10^{16} cm^{-3} to 10^{14} cm^{-3}, the efficiency is increased from 13.40% to 17.91% entirely due to the increased J_{sc} from 21.87 mA to 28.95 mA.

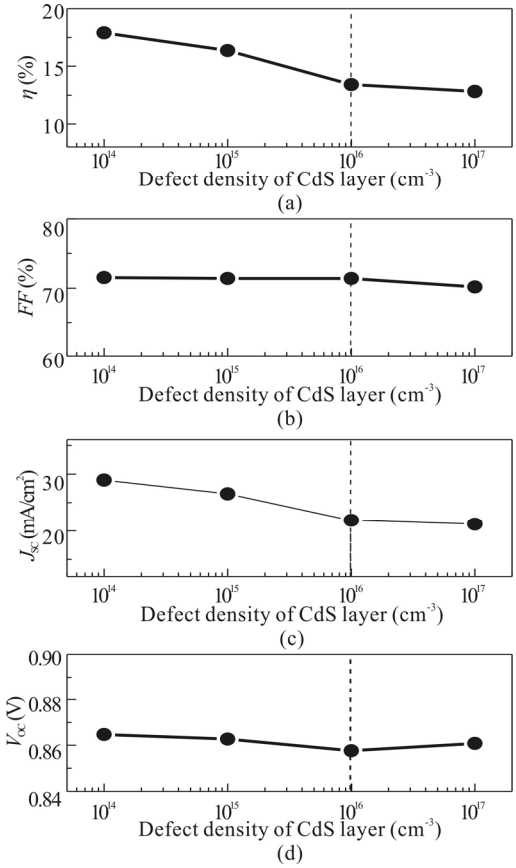

Fig.4 Defect density effect of CdS window layer on solar cell parameters

The improvement of FF and V_{OC} for the advanced model can be principally attributed to the decrease of defect density of CdTe films and the increased metal work function of back contact. The expressions for V_{OC} and FF are

$$V_{OC} = \frac{nkT}{q} \ln\left(\frac{J_{SC}}{J_0} + 1\right), \tag{1}$$

$$FF = \frac{V_{max} \times J_{max}}{V_{OC} \times J_{SC}}. \tag{2}$$

As illustrated in Fig.5, the performance parameters of CdTe solar cells are all deteriorated with the increase of the defect density of CdTe films. The reduction of defect density in CdTe films is considered to account for the enhancement of all output parameters of CdTe solar cell. The highest conversion efficiency around 18.79% with V_{OC}=0.88 V, J_{SC}=26.63 mA/cm^2 and FF=79.73% can be found for defect density of 10^{12} cm^{-3}. In addition, for back contact barrier, it is shown via several modeling efforts that the back contact energy can also affect V_{OC}. Depending on the doping levels in CdTe, the band bending (and therefore V_{OC}) in this layer can be determined by the energy of back contact. Therefore, large work function contact materials can also lead to improved V_{OC}.

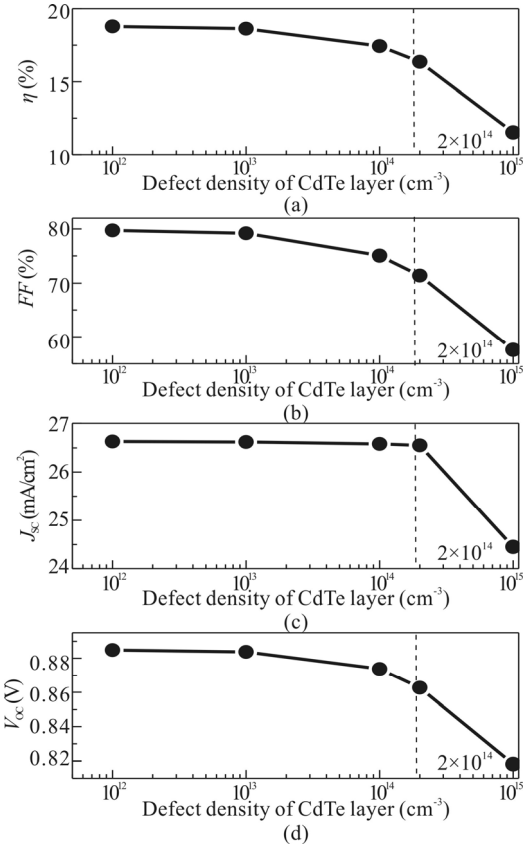

Fig.5 Defect density effect of CdTe absorbing layer on solar cell parameters

Metal work function Φ_m (for majority carriers) can be input by the user. However, the user can also choose the option "flat bands". In this case, SCAPS-1D calculates the metal work function Φ_m for every temperature in such a way that flat band conditions prevail. When the layer adjacent to the contact is a n-type, the metal work function Φ_m is expressed as

$$\Phi_m = \chi + k_B T \ln\left(\frac{N_C}{N_D + N_A}\right). \quad (3)$$

and when it is a p-type, Φ_m is expressed as [16]

$$\Phi_m = \chi + E_g - k_B T \ln\left(\frac{N_C}{N_A - N_D}\right). \quad (4)$$

Simulations are done by using silver (Ag), iron (Fe), niobium (Nb), copper (Cu) graphite alloy, nickel (Ni) and platinum (Pt), and they are back contact of CdTe solar cell. The influence of the metal work function on the performance of solar cell is illustrated in Fig.6 and Tab.2.

There are two types of junction depending on the nature of metal with the work function Φ_m of CdTe film with energy band of 1.5 eV and electronic affinity of 3.9 eV. If Φ_m<5.4 eV, the junction behaves like a Schottky barrier, but if $\Phi_m \geq 5.4$ eV, the junction behaves as an ohmic contact. The stability of the back contact in the solar cell is necessary for good performance.

It's clear in Fig.6 that when the metal work function increases, V_{OC} is increased. Thus, the efficiency of CdTe solar cell also can be increased. From Tab.2, it can be concluded that efficiency of the proposed solar cell increases from 4.74 eV to 5.70 eV with the increase of metal work function.

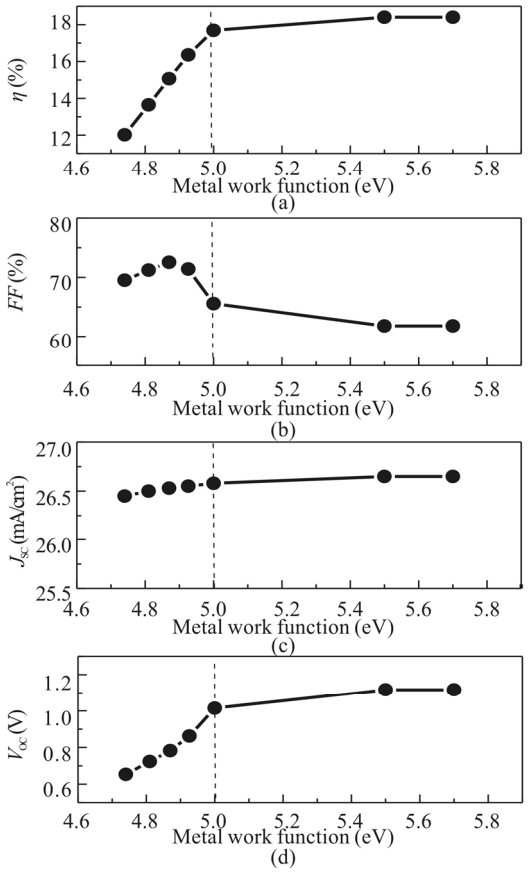

Fig.6 Metal work function effect on solar cell parameters

Tab.2 Efficiency and metal work function of the solar cells with different metals

Metal	Ag	Fe	Nb	Cu	Ni	Pt
Φ_m (eV)	4.74	4.81	4.87	5.00	5.50	5.70
η (%)	12.02	13.65	15.07	17.69	18.40	18.40

After the previous results, we note that there is more than one parameter to influence the performance of solar cell. Then after several estimations, we find the current density-voltage characteristic of the modified solar cell with AZO is almost confused with those obtained by Gupta and Compaan[9] with the same thickness.

The modifications made to the structure (b) (Fig.1 (b)) to find these results are taken. The same thickness is taken by Gupta[9], i.e., 0.7-μm-thick AZO, 0.13-μm-thick CdS and 1.3-μm-thick CdTe, and the electrical properties are the same in Tab.1, except that the defect density (N_{AG}) for the CdS layer is 1.2×10^{15} cm^{-3}, the mobility of the holes for the CdTe absorbing layer is 80 cm^2/Vs, the acceptor concentration (hole density p) is 2×10^{15} cm^{-3}, and the defect density (N_{DG}) is 1×10^{15} cm^{-3}. Finally, the back

contact is 4.8 eV. Even small variations can be seen to influence the performance of the solar cell.

Fig.7 shows the current density-voltage curves of ZnO:Al/CdS/CdTe solar cells in experiment[9] and simulation by SCAPS-1D, where AM 1.5G condition are both used. The trend in simulation agrees well with that in the experiment.

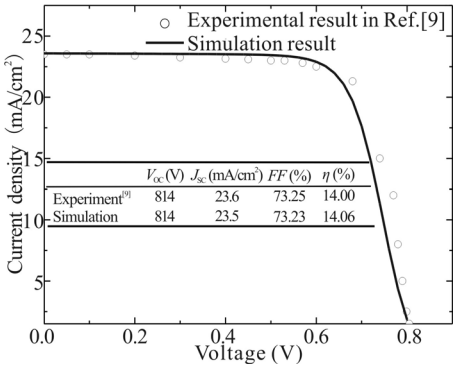

Fig.7 The computed and observed current density-voltage curves of AZO/CdS/CdTe solar cells

In recent years, the research evolves towards decreasing the cost of production and the consuming time of the CdS/CdTe solar cell by manufacturing thinner cells. Generally, reducing the thickness of absorbing layer in the typical CdTe solar cell from larger than 4 μm to 1 μm can save more than 75% of the CdTe material. Then if the film deposition rate can be maintained, the time of deposit and energy can be at least four times lower. For example, when the thickness of CdTe absorber is reduced from 4 μm to 1 μm, the deposition time is decreased from one hour to only 15 min, and the required energy is also decreased at the same rate[13].

Theoretically, the minimum thickness required for CdTe films to absorb 99% incident photons with energy greater than E_g is approximately 1—2 μm[8,17]. The solar cells, whose thickness of absorption layer is less than 1 μm, are semi-transparent for the majority of wavelengths in the solar spectrum, and the losses of photogenerated current associated with this transparency are above the gap of the semiconductor known as losses of deep penetration. In order to reduce the possible recombination loss and the barrier height at the back contact of ultrathin (1 μm) CdTe cell, a low bandgap material PbTe with E_g=0.29 eV was inserted at the back to reduce back surface recombination rate at the CdTe/PbTe heterojunction. This low bandgap material can act as a BSF to bounce back the carriers (electrons) from the CdTe/PbTe junction, which can contribute in the enhancement of carriers. Fig.1(c) shows the structure of the modified solar cell, which is composed of 500-nm-thick ZnO:Al, 30-nm-thick CdS, 1-μm-thick CdTe and 0.1-μm-thick PbTe BSF. The band diagram of this ultrathin cell with small bandgap of PbTe (0.29 eV) is illustrated in Fig.8. The interface of the heterojunction iso-type p-CdTe/p-PbTe shows a discontinuity of the conduction bands ΔE_C of 0.7 eV and the valence bands ΔE_V of 1.21 eV.

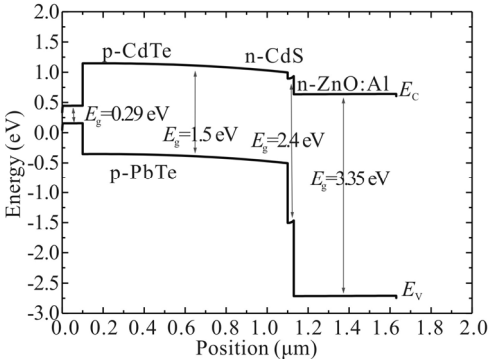

Fig.8 Band diagram of CdTe solar cells with PbTe BSF

Fig.9 shows the current density-voltage curves of the CdTe solar cells with and without PbTe BSF for different back metal work functions by using two methods. In the first method, as show in Fig.9(a), choose the option "flat bands", i.e., the back metal work function is fixed at 4.92 eV. We note that the solar cell with PbTe BSF can achieve the higher current. After adding PbTe BSF, the efficiency is increased from 15.02% to 19.28% entirely due to the increased V_{OC} from 0.67 V to 0.88 V. *FF* is strongly affected, but J_{SC} is only improved a bit due to reduced minority carrier recombination loss at the back contact. In the second method, as show in Fig.9(b), do not chosen flat band, SCAPS-1D calculates the metal work function, i.e., the metal work function for the cell without BSF layer is 4.87 eV, and that for the cell with PbTe BSF layer is 5.04 eV. The results for the cell with PbTe in Fig.9(b) are almost the same with those in Fig.9(a), but the performance of cell without BSF in Fig.9(b) is decreased compared with that in Fig.9(a) due to the reduced metal work function.

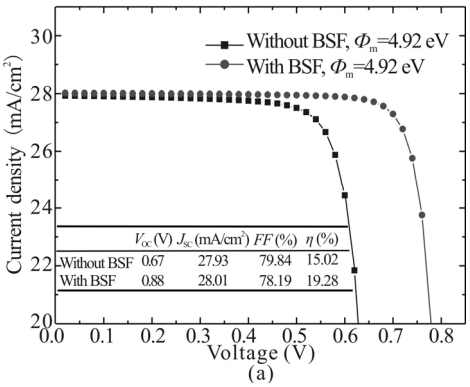

Fig.9 Current-voltage curves of CdTe solar cells on ZnO:Al and 1-μm-thick CdTe with and without PbTe BSF with (a) fixed and (b) varied back metal work functions

In conclusion, we investigate the influence of parameters of the individual layers on the performances of CdTe solar cell thin film under illumination AM 1.5G using SCAPS-1D. A baseline model with SnO_2:F and a modified model with ZnO:Al can achieve the efficiencies of 15.14% and 16.36%, respectively. The efficiency improvement of the cell with ZnO:Al TCO is primarily contributed by the increased J_{SC} by the reduction of thickness and defect density for CdS layer, and the improvements of *FF* and V_{OC} can be principally attributed to the decrease of defect density of CdTe films and the increased metal work function of back contact. Even small variations can be seen to influence the performance of the cell. For decreasing the cost of CdTe solar cell production by using 1-μm-thick CdTe absorbing layer, a PbTe BSF layer (0.1μm) is introduced between 1-μm-thick CdTe absorbing layer and back contact of the cell, and the efficiency of this thinner solar cell is improved. The efficiency of thinner cell with PbTe BSF layer is 19.28%, which is higher than that of typical model with 4-μm-thick CdTe film.

References

[1] Sze S., Physics of Semiconductor Devices, 2nd ed., Wiley, New York, 1981.

[2] Green M. A., Emery K., Hishikawa Y. and Watra W., Progress in Photovoltaics: Research and Applications **18**, 144 (2010).

[3] Green M. A., Hishikawa Y., Watra W., Dunlop E. D., Levi D. H., Hohl-Ebinger J. and Ho-Bailie A. W. Y., Progress in Photovoltaics: Research and Applications **25**, 668 (2017).

[4] Burgelman M., Verschraegen J., Degrave S. and Nollet P., Progress in Photovoltaics: Research and Applications **12**, 143 (2003).

[5] Amin N., Sopian K. and Konagai M., Solar Energy Materials and Solar Cells **91**, 1202 (2007).

[6] Huang C.H. and Chuang W.J., Vacuum **118**, 32 (2015).

[7] J. Britt and C. Ferekides, Applied Physics Letters **62**, 2851 (1993).

[8] Xuanzhi Wu, Solar Energy **77**, 803 (2004).

[9] Gupta A. and Compaan A.D., Applied Physics Letters **85**, 684 (2004).

[10] Khosroabadi S. and Keshmiri S. H., Optics Express **22**, A921 (2014).

[11] M. Burgelman, P. Nollet and S. Degrave, Thin Solid Films **361-362**, 527 (2000).

[12] Gloeckler M., Fahrenbruch A.L. and Sites J.R., Numerical Modeling of CIGS and CdTe Solar Cells: Setting the Baseline, 3rd World Conference on Photovoltaic Energy Conversion, (2003).

[13] M. A. Matin and Mrinmoy Dey, High Performance Ultra-Thin CdTe Solar Cell with Lead Telluride BSF, 3rd International Conference on Informatics, Electronics & Vision, (2014).

[14] Takiguchi Y. and Miyajima S., Japanese Journal of Applied Physics **54**, 112303 (2015).

[15] Ting L. Chu and Shirley S. Chu, Progress in Photovoltaics: Research and Applications **1**, 31 (1993).

[16] Burgelman M., Decock K., Niemegeers A., Verschraegen J. and Degrave S., SCAPS Manual, (2016).

[17] Amin N., Isaka T., Okamoto T., Yamada A. and Konaga M., Japanese Journal of Applied Physics **38**, 4666 (1999).